s-wave positron-hydrogen scattering via Faddeev equations: Elastic scattering and positronium formation

Andrei A. Kvitsinsky,* Jaume Carbonell, and Claude Gignoux
Institut des Sciences Nucléaires, 53 avenue des Martyrs, 38026 Grenoble, France
(Received 27 September 1993; revised manuscript received 22 August 1994)

s-wave scattering of positrons on atomic hydrogen is treated by solving the Faddeev equations. Elastic phase shifts below the Ps($n = 1$) excitation threshold and the K-matrix elements within the ore gap between the Ps($n = 1$) and H($n = 2$) thresholds are calculated as well as the zero-energy 2γ annihilation rate of the $e^+ e^-$ pair.

PACS number(s): 34.80.Bm, 11.80.Jy, 36.10.Dr, 03.65.Nk

I. INTRODUCTION

This paper deals with the s-wave scattering of positron on atomic hydrogen below the first excitation threshold ($n = 2$) of hydrogen. In this case the possible reactions are

$$e^+ + \mathrm{H} \rightarrow \begin{cases} e^+ + \mathrm{H} & \text{elastic scattering} \\ \mathrm{Ps} + p & \text{positronium formation.} \end{cases} \quad (1)$$

Positronium formation occurs when the energy of the incident positron is in the ore gap, i.e., between the Ps($n = 1$) and H($n = 2$) thresholds. The general interest in studying the positron-atom collisions is due to experimental activity in this field that has been developed in recent years with the advent of low-energy positron beams and the possibility of measuring simple systems [1–3]. The e^++H system provides the simplest example of this kind and is an ideal test point for various theoretical methods solving scattering problems.

In addition, it is worth studying for its own sake due to features that distinguish it from the classical problem of e^--H scattering. This is a full three-particle Coulomb problem where all particles are distinct so that there are no exchange effects, rearrangement of the target (positronium formation) is possible, the role of long-range polarization force in the channel Ps+p is quite essential near the positronium formation threshold, etc. Another feature of interest, with no counterpart in electron-atom collisions, is the annihilation of the $e^+ e^-$ pair.

Previously, the low-energy e^--H scattering has been calculated by means of the Kohn variational principle [4–7]. The corresponding results are the most accurate and reliable among many other approximative estimates. The elastic phase shifts now seem to be firmly established. However, some uncertainties remain, especially regarding the positronium formation cross section for which sensibly different results were obtained. We refer to [8,9] for an up to date review.

Most of the methods used are based on variational principles. To our knowledge only one work [10] obtained a direct solution of the e^--H scattering problem, still limited to the elastic region ($0.1 < k < 0.70$). Because of great interest this reaction attracts in positronium physics, and in view of recent reports of possible experimental measures of the Ps formation cross sections [2,3], we find it worthwhile to solve the problem via a completely different technique that provides a direct solution of three-body dynamical equations. Namely, we present here a solution of the Faddeev equations in configuration space, in a continuing effort [11,12] to develop the Faddeev approach in atomic physics.

The Faddeev approach has been widely used in nuclear physics problems, but it has been applied only very recently to atomic three-body scattering problems [12,13] on the basis of the so-called modified Faddeev equations due to Merkuriev [14]. There are two different ways to solve these equations numerically. One of them, exploited in Ref. [12] for the e^--Ps scattering problem, uses a bipolar expansion [17] of the Faddeev amplitude. Another method, developed in Ref. [13], is based on the total-angular-momentum representation [18] and consists of a direct solution of the corresponding three-dimensional equations. In this paper we adopt the bipolar expansion method of Ref. [12] with considerable improvements in the numerical part.

II. FADDEEV EQUATIONS

A. Kinematics

The particles of the $e^+ + (pe^-)$ system are numerated by the label α=1,2,3: $(e^+, p, e^-) = (1, 2, 3)$. We shall use the atomic units (a.u.) $\hbar^2 = e^2 = m_e = 1$, so that the length unit is the Bohr radius a_0.

The configuration space of the system is described by three sets of the mass-scaled Jacobi vectors $\{\mathbf{x}_\alpha, \mathbf{y}_\alpha\}$, which are related to the position vectors of the particles $\mathbf{r}_\alpha$ by

*Permanent address: Department of Mathematical and Computational Physics, Institute for Physics, University of St. Petersburg, St. Petersburg 198904, Russia.

$$\mathbf{x}_\alpha = -\left[\frac{2m_\beta m_\gamma}{m_\beta + m_\gamma}\right]^{1/2} (\mathbf{r}_\beta - \mathbf{r}_\gamma) \ , \tag{2}$$

$$\mathbf{y}_\alpha = \left[\frac{2m_\alpha (m_\beta + m_\gamma)}{M}\right]^{1/2} \left(\mathbf{r}_\alpha - \frac{m_\beta \mathbf{r}_\beta + m_\gamma \mathbf{r}_\gamma}{m_\beta + m_\gamma}\right) , \tag{3}$$

where triplets $(\alpha\beta\gamma)$ are cyclic permutations of (123), m_α are particle masses, and M is the total mass. The Jacobi vectors with different α's are related by an orthogonal transform

$$\mathbf{x}_\beta = c_{\beta\alpha}\mathbf{x}_\alpha + s_{\beta\alpha}\mathbf{y}_\alpha, \ \mathbf{y}_\beta = -s_{\beta\alpha}\mathbf{x}_\alpha + c_{\beta\alpha}\mathbf{y}_\alpha \ . \tag{4}$$

Here the coefficients are expressed through the masses of the particles

$$c_{\beta\alpha} = -\left[\frac{m_\beta m_\alpha}{(M - m_\beta)(M - m_\alpha)}\right]^{1/2} ,$$

$$s_{\beta\alpha} = (-1)^{\beta-\alpha} \operatorname{sgn}(\alpha - \beta) \left(1 - c_{\beta\alpha}^2\right)^{1/2}$$

and satisfy $c_{\beta\alpha}^2 + s_{\beta\alpha}^2 = 1$. Note that in the limit $m_e/m_p \to 0$ ($m_1/m_2 = m_3/m_2 \to 0$) the scaled Jacobi vectors (2) with α=1,2 become

$$\mathbf{x}_1 \simeq \sqrt{2}\,(\mathbf{r}_{e^-} - \mathbf{r}_p) \ , \ \mathbf{x}_2 \simeq (\mathbf{r}_{e^+} - \mathbf{r}_{e^-}) \ ,$$

$$\mathbf{y}_1 \simeq \sqrt{2}\,(\mathbf{r}_{e^+} - \mathbf{r}_p) \ , \ \mathbf{y}_2 \simeq 2\left[\mathbf{r}_p - \frac{1}{2}(\mathbf{r}_{e^+} + \mathbf{r}_{e^-})\right] \tag{5}$$

and the coefficients of (4) are simplified to

$$c_{12} = c_{21} \simeq s_{12} = -s_{21} \simeq -\frac{1}{\sqrt{2}} \ . \tag{6}$$

Although we shall not use the approximation $m_e/m_p = 0$, it is useful to keep in mind the approximative relations (5) of the Jacobi coordinates with physical distances in the system.

The three-body dynamics at fixed total angular momentum L is constrained onto a three-dimensional internal space [18]. For local coordinates on the internal space we use

$$x_\alpha = |\mathbf{x}_\alpha| \ , \ y_\alpha = |\mathbf{y}_\alpha| \ , \ u_\alpha = (\hat{\mathbf{x}}_\alpha, \hat{\mathbf{y}}_\alpha) \ ,$$

where $\hat{\mathbf{x}} = \mathbf{x}/|\mathbf{x}|$. Due to Eqs. (2) and (3), these coordinates are related by

$$x_\beta = \left[c_{\beta\alpha}^2 x_\alpha^2 + s_{\beta\alpha}^2 y_\alpha^2 + 2c_{\beta\alpha}s_{\beta\alpha}x_\alpha y_\alpha u_\alpha\right]^{1/2} ,$$

$$y_\beta = \left[s_{\beta\alpha}^2 x_\alpha^2 + c_{\beta\alpha}^2 y_\alpha^2 - 2c_{\beta\alpha}s_{\beta\alpha}x_\alpha y_\alpha u_\alpha\right]^{1/2} ,$$

$$x_\beta\, y_\beta\, u_\beta = \left(c_{\beta\alpha}^2 - s_{\beta\alpha}^2\right) x_\alpha\, y_\alpha\, u_\alpha - c_{\beta\alpha}\, s_{\beta\alpha}\left(x_\alpha^2 - y_\alpha^2\right) . \tag{7}$$

B. Modified Faddeev equations

The s-wave (L=0) Hamiltonian of the three-body Coulomb system is of the form [18]

$$H = H_0 + \sum_\alpha V_\alpha(x_\alpha) \ , \tag{8}$$

where V_α stand for the Coulomb potentials

$$V_\alpha(x_\alpha) = \frac{z_\beta z_\gamma}{x_\alpha}\left[\frac{2m_\beta m_\gamma}{m_\beta + m_\gamma}\right]^{1/2} ,$$

z_β are the particle charges, and the indices $(\alpha\beta\gamma)$ are related as in Eqs. (2) and (3). The kinetic-energy operator H_0 is given by

$$H_0 = -x_\alpha^{-2}\partial_{x_\alpha} x_\alpha^2 \partial_{x_\alpha} - y_\alpha^{-2}\partial_{y_\alpha} y_\alpha^2 \partial_{y_\alpha} + \left(\frac{1}{x_\alpha^2} + \frac{1}{y_\alpha^2}\right)\hat{l}_\alpha^2 \ , \tag{9}$$

$$\hat{l}_\alpha^2 = -\partial_{u_\alpha}\left(1 - u_\alpha^2\right)\partial_{u_\alpha} \ . \tag{10}$$

The modified Faddeev equations for the Hamiltonian (8) are built up along a cutoff procedure due to Merkuriev [14]. Namely, Coulomb potentials are decomposed into short- and long-range parts

$$\begin{aligned} V^{(s)}(x_\alpha, y_\alpha) &= V_\alpha(x_\alpha)\,\zeta_\alpha(x_\alpha, y_\alpha) \ , \\ V^{(l)}(x_\alpha, y_\alpha) &= V_\alpha(x_\alpha)\left[1 - \zeta_\alpha(x_\alpha, y_\alpha)\right] \end{aligned} \tag{11}$$

by means of a cutoff function ζ_α that vanishes asymptotically in the so-called three-body region (where $x_\alpha \sim y_\alpha \to \infty$) and tends to one in the corresponding two-body region (where $x_\alpha \ll y_\alpha \to \infty$). We exploit the same form of the cutoff as in the previous works [12,13]:

$$\zeta_\alpha(x, y) = 2\left\{1 + \exp\left[\frac{(x/x_0)^\nu}{y/y_0 + 1}\right]\right\}^{-1} ,$$

with the same set of the cutoff parameters ν=2.3, x_0=2, y_0=10. In general, one should take $\nu > 2$ and the other parameters are rather arbitrary.

In terms of the screened potentials (11) the modified Faddeev equations read

$$\left(H_{as} + V_\alpha^{(s)} - E\right)\Psi_\alpha = -V_\alpha^{(s)} \sum_{\beta\neq\alpha} \Psi_\beta, \tag{12}$$

where the operator H_{as} incorporates the long-pange parts of the Coulomb potentials

$$H_{as} = H_0 + \sum_\alpha V_\alpha^{(l)}$$

and the total wave function is the sum of the Faddeev components

$$\Psi = \sum_\alpha \Psi_\alpha$$

The set (12) involves three equations. As shown in [13], one can reduce this number to two by choosing $\zeta_3 \equiv 0$ for the cutoff function in the channel $\alpha = 3$, involving the repulsive pair e^+ p. From that follows $\Psi_3 = 0$ and one is left with a set of two equations for the components Ψ_1, Ψ_2:

$$\left[H_0 + V_\alpha(x) + V_3(x_{3\alpha}) + V_\beta^{(l)}(x_{\beta\alpha}, y_{\beta\alpha}) - E\right]$$

$$\times \Psi_\alpha(x, y, u) = -V_\alpha^{(s)}(x, y)\Psi_\beta(x_{\beta\alpha}, y_{\beta\alpha}, u_{\beta\alpha}) \tag{13}$$

where α,β=1,2 and $\beta \neq \alpha$; $x_{\beta\alpha}$, $y_{\beta\alpha}$, and $u_{\beta\alpha}$ stand for the coordinates x_β, y_β, and u_β expressed through $x_\alpha \equiv x$, $y_\alpha \equiv y$, and $u_\alpha \equiv u$ according to (7).

C. Asymptotics

Equations (13) are the starting point of our approach. For scattering problems, they should be supplemented with appropriate asymptotic boundary conditions. Below the Ps($n = 1$) threshold only the elastic channel is open and the asymptotics of the Faddeev components are

$$\Psi_1(x,y,u)|_{y\to\infty} \sim \frac{1}{xy}\,\varphi_{\rm H}(x)\,[\sin q_1 y + \tan\delta \cos q_1 y]\ ,$$
$$\Psi_2(x,y,u)|_{y\to\infty} \sim 0\,, \tag{14}$$

where $\varphi_{\rm H}(x)$ is the hydrogen ground-state radial wave function, δ is the phase shift, and q_1 is the momentum of incident positron conjugate to coordinate y_1.

In the ore gap, i.e., between the Ps($n = 1$) and H($n = 2$) thresholds, two asymptotic channels are open. In this case we make use of the K-matrix setting. Namely, we look for two independent solutions of (13) corresponding to different initial states of the system: (i) The first solution

$$\Psi_1(x,y,u)|_{y\to\infty} \sim \frac{1}{xy}\,\varphi_{\rm H}(x)\,[\sin q_1 y + K_{11}\cos q_1 y]\ , \tag{15}$$

$$\Psi_2(x,y,u)|_{y\to\infty} \sim \frac{1}{xy}\,\varphi_{\rm Ps}(x)\sqrt{\frac{q_1}{q_2}}\,K_{21}\cos q_2 y\,, \tag{16}$$

where $\varphi_{\rm Ps}$ is the positronium ground-state radial wave function. (ii) The second solution

$$\Psi_1(x,y,u)|_{y\to\infty} \sim \frac{1}{xy}\,\varphi_{\rm H}(x)\sqrt{\frac{q_2}{q_1}}K_{12}\cos q_1 y\,, \tag{17}$$

$$\Psi_2(x,y,u)|_{y\to\infty} \sim \frac{1}{xy}\,\varphi_{\rm Ps}(x)\,[\sin q_2 y + K_{22}\cos q_2 y]\ , \tag{18}$$

where q_α are corresponding mass-scaled momenta

$$E = -\frac{1}{2} + q_1^2 = -\frac{1}{4} + q_2^2 \ \text{(a.u.)}$$

related to the physical momenta k_α in the system according to Eq. (3)

$$k_\alpha = q_\alpha\sqrt{2m_\alpha\left(1-\frac{m_\alpha}{M}\right)}\ ,\ \alpha = 1,2\ , \tag{19}$$

so that k_1 and k_2 are the momenta of the positron and positronium atom, respectively. The atomic wave functions in Eqs. (16)–(18) are normalized by

$$\int_0^\infty \varphi_{\rm H}^2(x)dx = \int_0^\infty \varphi_{\rm Ps}^2(x)dx = 1\ .$$

The s-wave cross section for scattering between channels α and β is expressed in terms of the K-matrix elements as

$$\sigma_{\alpha\beta} = \frac{4\pi a_0^2}{k_\alpha^2}\left|\left(\frac{K}{1-iK}\right)_{\alpha\beta}\right|^2\ . \tag{20}$$

As seen from Eqs. (16)–(18), outgoing waves with different clusterization of particles are distributed among different Faddeev components, so that each component contains only one two-body bound state. This allows one to set up asymptotic boundary conditions for the components using the corresponding set of Jacobi coordinates perfectly designed for this purpose. This is one of the principal merits of the Faddeev approach. Note that asymptotic decoupling of channels is due to the cutoff in the short-range potentials $V_\alpha^{(s)}$ on the right-hand side of Eq. (13): The terms $V_\alpha^{(s)}\Psi_\beta$ vanish sufficiently fast in the three-body region due to the structure of the cutoff (11).

D. Positron-electron annihilation

Annihilation of the e^+e^- pair in the e^++H scattering is either for two or three photons, depending on the spin of the pair. Here we are interested in the singlet 2γ annihilation that yields a dominant contribution into the overall rate and under certain assumptions [8] may be written as $\lambda = \pi r_0^2 c Z_{\rm eff}$, where r_0 is the classical radius of electron, c is the speed of light,

$$Z_{\rm eff} = \int_0^\infty |\Psi\,(\mathbf{r}_{e^+} = \mathbf{r}_{e^-}\,;\,r_p)|^2\,\rho^2 d\rho$$

is the effective electron density near the positron, and ρ is the proton distance to the e^+e^- center of mass. Expressed in terms of the Faddeev components, normalized according to (14) below Ps(n=1) threshold, it takes the form

$$Z_{\rm eff} = 2\left[\frac{m_2\,M}{(m_2+m_1)\,(m_2+m_3)}\right]^{3/2} \times |c_{12}|^3\int_0^\infty [\Psi_1+\Psi_2]^2\,|_{x_2=0}\,y_2^2\,dy_2\ . \tag{21}$$

The factor in front of the integral comes from relations (2) and (3) between Jacobi coordinates and position vectors of the particles.

III. BIPOLAR EXPANSION AND NUMERICAL METHOD

To solve Eqs. (13) numerically, the Faddeev components are decomposed into the bipolar basis. This method has been extensively exploited in the trinucleon problem [17–19], in the Coulomb three-body bound-state problem [20], and in our previous work on e^--Ps scattering [12]. In the case of $L = 0$, the corresponding bases are the normalized Legendre polynomials $\tilde{P}_l(u) = \sqrt{l+1/2}\,P_l(u)$, eigenfunctions of the operator (10):

$$\Psi_\alpha(x,y,u) = \frac{1}{xy}\sum_{l_\alpha=0}^{\infty} F_{l_\alpha}^{(\alpha)}(x,y)\tilde{P}_{l_\alpha}(u)\ . \tag{22}$$

Substituting this into (13) yields an infinite set of two-dimensional integrodifferential equations for the partial Faddeev components:

$$(-\Delta_{l_\alpha} + V_\alpha - E)\, F_{l_\alpha}^{(\alpha)} + \sum_{l'_\alpha} W_{l_\alpha l'_\alpha}^{(\alpha)} F_{l'_\alpha}^{(\alpha)} = -V_\alpha^{(s)} \sum_{l_\beta} \hat{h}_{l_\alpha l_\beta}^{\beta\alpha} F_{l_\beta}^{(\beta)} \ , \quad (23)$$

where $\alpha, \beta = 1, 2$ and $\beta \neq \alpha$; $(-\Delta_l)$ are the partial components of the kinetic-energy operator (10):

$$-\Delta_l = -\partial_x^2 - \partial_y^2 + l(l+1)\left[\frac{1}{x^2} + \frac{1}{y^2}\right] .$$

The coupling through the functions $W_{ll'}^{(\alpha)}$ is due to long range potentials V_3 and $V_\beta^{(l)}$ of Eqs. (13),

$$W_{ll'}^{(\alpha)}(x,y) = \int_{-1}^{1} du \tilde{P}_l(u)\tilde{P}_{l'}(u) \times \left[V_3\left(x_{3\alpha}\right) + V_\beta^{(l)}\left(x_{\beta\alpha}, y_{\beta\alpha}\right)\right] , \quad \beta \neq \alpha \ . \quad (24)$$

The operator $\hat{h}_{l_\alpha l_\beta}^{(\beta\alpha)}$ provides integral coupling of the partial components

$$\left[\hat{h}_{l_\alpha l_\beta}^{(\beta\alpha)} F\right](x,y) = \int_{-1}^{1} du \frac{xy}{x_{\beta\alpha} y_{\beta\alpha}} \tilde{P}_{l_\alpha}(u)\tilde{P}_{l_\beta}\left(u_{\beta\alpha}\right) \times F\left(x_{\beta\alpha}, y_{\beta\alpha}\right) \ , \quad (25)$$

where $x_{\beta\alpha}(x,y,u)$, $y_{\beta\alpha}(x,y,u)$, and $u_{\beta\alpha}(x,y,u)$ are functions defined by Eqs. (7) with $x_\alpha \equiv x$, $y_\alpha \equiv y$, and $u_\alpha \equiv u$.

Equations (23) are subject to the regular boundary conditions

$$F_{l_\alpha}^{(\alpha)}(x=0,y) = F_{l_\alpha}^{(\alpha)}(x,y=0) = 0 \quad (26)$$

$$F_{l_\alpha}^{(\alpha)}(x=\infty,y) = 0 \quad (27)$$

and the asymptotic conditions at $y \to \infty$ which follow from (14) or (16)–(18).

Let us consider, for instance, the scattering within the ore gap. Then Eqs. (16)–(18) in terms of the partial Faddeev components become (i) the first solution

$$F_{l_1}^{(1)}(x, y \to \infty) \sim \delta_{l_1 0}\, \varphi_{\mathrm{H}}(x) \left[\sin q_1 y + K_{11} \cos q_1 y\right] , \quad (28)$$

$$F_{l_2}^{(2)}(x, y \to \infty) \sim \delta_{l_2 0}\, \varphi_{\mathrm{Ps}}(x) \sqrt{\frac{q_1}{q_2}}\, K_{21} \cos q_2 y \, , \quad (29)$$

and (ii) the second solution

$$F_{l_1}^{(1)}(x, y \to \infty) \sim \delta_{l_1 0}\, \varphi_{\mathrm{H}}(x) \sqrt{q_2/q_1}\, K_{12} \cos q_1 y \, , \quad (30)$$

$$F_{l_2}^{(2)}(x, y \to \infty) \sim \delta_{l_2 0}\, \varphi_{\mathrm{Ps}}(x) \left[\sin q_2 y + K_{22} \cos q_2 y\right] . \quad (31)$$

Consider the effective density (21) of the 2γ annihilation of the $e^+ e^-$ pair. In terms of the partial Faddeev components it is written as

$$Z_{\mathrm{eff}} = \int_0^\infty dy_2\, \omega(y_2) \ ,$$

with the density distribution

$$\omega(y) = \left[\frac{m_2 M}{(m_2+m_1)(m_2+m_3)}\right]^{3/2} |c_{12}|^3 \times \left\{ \frac{1}{|s_{12} c_{12}|\, y} \sum_{l_1=0}^{\infty} \sqrt{2l_1+1} F_{l_1}^{(1)}\left(|s_{12}|\, y, |c_{12}|\, y\right) + \partial_x F_{l_2=0}^{(2)}(x=0,y) \right\}^2 . \quad (32)$$

Our numerical method in solving Eqs. (23) makes use of a spline expansion of the partial Faddeev components

$$F_{l_\alpha}^{(\alpha)}(x,y) = \sum_{m=1}^{2N_x} \sum_{n=1}^{2N_y} f_{mn}^{(\alpha l_\alpha)} s_m(x) s_n(y) \ , \quad (33)$$

where s_i are the cubic Hermite polynomial splines [21]. The number of splines is twice the number of subintervals on which one divides the domain of corresponding variables. Upon substituting the spline expansion into Eqs. (23), the problem is discretized by means of orthogonal collocation procedure [22].

The potentials (24) and the integral terms (25) are calculated by the Gauss quadrature formula with N_W and N_g points, respectively. The resulting algebraic equation for the coefficients of Eqs. (33) is solved by a direct matrix inversion with dimension $4\, N_c\, N_x\, N_y$, where $N_c = N_1 + N_2$ is the number of partial channels $\{l_1\}, \{l_2\}$ of Eqs. (23) taken into account.

We made use of rectangular nonuniform grids $G = G_x \times G_y$, where $G_q = \{q_0, q_1, \ldots, q_N\}$ is a set of $N+1$ nonequidistant knots. They are defined by means of the accelerator $A_q = q_{i+1} - q_i$ so that the grid step increases by A_q when passing to next subinterval. A grid $G_{q=x,y}$ is thus characterized by the triplet $\{N; A_q; q_{\max}\}$.

The zero boundary conditions (26) and (27) and the asymptotic boundary conditions (28)–(31) are implied for $x = x_{\max}$ and $y = y_{\max}$, respectively, with $x_{\max}$ and $y_{\max}$ large enough. Let us explain in more detail the asymptotic boundary conditions when two open channels are taken into account. Instead of implying the conditions (28)–(31), we look for two solutions to the Faddeev equations (23) ${}^1F_{l_\alpha}^{(\alpha)}$ and ${}^2F_{l_\alpha}^{(\alpha)}$ subject to the conditions

$${}^1F_{l_\alpha}^{(\alpha)}(x, y=y_{\max}) = \delta_{\alpha 1}\, \delta_{l_1 0}\, \varphi_{\mathrm{H}}(x) \ , \quad \alpha = 1,2 \quad (34)$$

$${}^2F_{l_\alpha}^{(\alpha)}(x, y=y_{\max}) = \delta_{\alpha 2}\, \delta_{l_2 0}\, \varphi_{\mathrm{Ps}}(x) \ , \quad \alpha = 1,2 \ . \quad (35)$$

Clearly, the physical solutions are linear combinations of these solutions. Let $F^{(1)} = \{F_{l_\alpha}^{(\alpha)}\}$ be the vector composed of the partial Faddeev components of the physical solution (28) and $F^{(2)}$ be that corresponding to (31). Let

${}^iF = \{{}^iF^{(\alpha)}_{l_\alpha}\}$ be similar vectors composed of solutions (34) and (35). Then

$$F^{(i)} = \lambda_{1i}\ {}^1F + \lambda_{2i}\ {}^2F \tag{36}$$

with $(i,j = 1,2)$

$$\lambda_{ij} = (\sin q_i y_{\max} + K_{ii}\cos q_i y_{\max})\,\delta_{ij} + (1-\delta_{ij})\sqrt{\frac{q_j}{q_i}}K_{ij}\cos q_i y_{\max}\ .$$

The derivatives of the solutions (34) and (35) satisfy

$$\partial_y\ {}^1F^{(\alpha)}_{l_\alpha}(x,y_{\max}) = \delta_{\alpha 1}\,\xi_{11}\,\delta_{l_1 0}\,\varphi_{\rm H}(x) + \delta_{\alpha 2}\,\xi_{21}\,\delta_{l_2 0}\,\varphi_{\rm Ps}(x)\ ,$$

$$\partial_y\ {}^2F^{(\alpha)}_{l_\alpha}(x,y_{\max}) = \delta_{\alpha 1}\,\xi_{12}\,\delta_{l_1 0}\,\varphi_{\rm H}(x) + \delta_{\alpha 2}\,\xi_{22}\,\delta_{l_2 0}\,\varphi_{\rm Ps}(x)\ ,$$

where the coefficients ξ_{ij} are constants, independent of x. Taking the y derivative of Eqs. (36) and (28)–(31) one gets a linear system for the K-matrix elements in terms of the coefficients ξ_{ij}.

IV. RESULTS

When solving numerically the Faddeev equations (23), the y-grid parameters must be properly adjusted for different energy regimes. At low energies, asymptotic oscillations in y of the Faddeev components are slow, so that the y grid should be dense at small distances and can be more sparse at large y. When the energy of the incident positron increases, the period of asymptotic oscillations decreases and the region of large y needs to be covered with a more dense grid. Also, at large energies Faddeev components reach their corresponding asymptotic limits at smaller y than for low energies, due to the essential role of long-range polarization potential at small energies. This remark concerns the parameter $y_{\max}$ of Eqs. (34) and (35): It should be large enough at low energies and can be decreased with an increase of energy.

The x grid was fixed once by ensuring a good description of the asymtotic states $\varphi_{\rm H}$ and $\varphi_{\rm Ps}$. Its parameters are $G_x = \{N_x = 12, A_x = 1.25, x_{\max} = 20\}$.

To fix an adequate y grid, we solved the problem by taking into account four partial channels $(l_1, l_2 = 0,1)$ and varying all grid parameters until a stability of the results within 0.1% is achieved. A typical grid for low energies $(k_1 < 0.1a_0^{-1})$ consists of $N_y = 18$ points with the acceleration factors $A_y = 1.25$ and $y_{\max} = 130$. For larger energies, $0.1a_0^{-1} \le k_1 \le 0.2a_0^{-1}$, a typical y grid is $G_y = \{N_y = 20, A_y = 1.22, y_{\max} = 70\}$ and for $k_1 > 0.2a_0^{-1}$, $G_y = \{20, 1.015, 40\}$.

A. Scattering length

Our first result concerns the scattering length. This quantity has been calculated very accurately by using variational methods [4,6] and provides a severe test for the Faddeev calculations. It provides also a direct check of the reliability of the wave function due to fact that in our approach the scattering parameters are directly extracted from the wave function without using any integral formula [23].

Table I presents the convergence of the e^+-H scattering length and the zero-energy effective density (21) of 2γ annihilation with an increasing number of bipolar harmonics $N_c = N_1 + N_2$ included in decompositions (22). The convergence is slow and nonmonotonous, as expected from the geometric asymmetry of the problem. A fully converged four digit quantity is obtained for $N_c = 14$ $(7+7)$. Grid parameters for the y variable are $G_y = \{10, 1.25, 40\}$, enlarged by six equidistant points up to $y_{\max} = 130$. The integrals (24) and (25) are, respectively, calculated with $N_W = 20$ and $N_g = 24$.

These results are obtained with $y_{\max} = 130$, but we have observed a sensible $y_{\max}$ dependence in the interval 40–250. This is due to the hydrogen polarizability effects. As is well known, they generate an effective long range interaction which in the adiabatic approximation results in a potential

$$V_p(r) = -\frac{1}{2}\frac{\alpha}{r^4}\ , \tag{37}$$

with $\alpha = 4.5$ and $r \approx \frac{y}{\sqrt{2}}$ the relative distance between the positron and the center of mass of the polarized H [see Eq. (5)]. This potential was included in the preceding variational calculations and its effects are indeed not negligible [4,6]. The value of α, well defined only in the framework of the adiabatic approximation, was considered as a free variational parameter and moved up to 4.8 in [6].

To obtain the scattering length corresponding to $y_{\max} = \infty$ we first fit its dependence on $y_{\max}$ and extrapolate. Results are presented in Fig. 1. The extrapolation has been done by assuming a law of the form

$$A(y_{\max}) = A_\infty + \frac{b_1}{y_{\max}} + \frac{b_2}{y^2_{\max}} + \cdots\ . \tag{38}$$

This assumption is supported by the numerical results

TABLE I. Convergence of the s-wave e^+-H scattering length A and $Z_{\rm eff}$ at zero energy; $\{l_1\}$ and $\{l_2\}$ are sets of partial angular momenta for the components Ψ_1 and Ψ_2 taken into account.

N_c	$\{l_1\}$	$\{l_2\}$	A	$Z_{\rm eff}$
4	01	01	-1.770	8.43
5	01	012	-2.111	9.30
6	012	012	-2.105	9.08
7	012	0123	-2.176	9.34
8	0123	0123	-2.148	9.13
10	01234	01234	-2.081	8.94
12	012345	012345	-2.071	8.93
14	0123456	0123456	-2.059	8.91
15	01234567	0123456	-2.059	8.91
16	01234567	01234567	-2.059	8.92

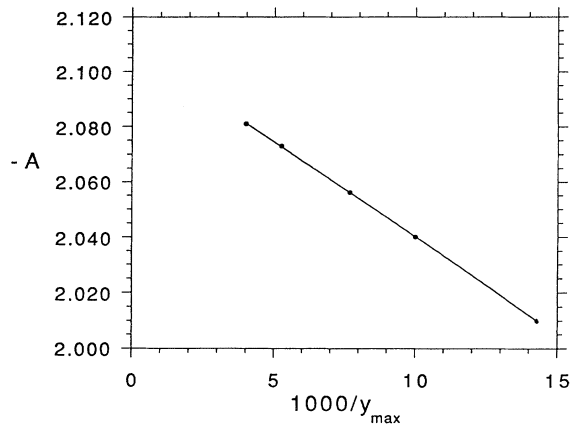

FIG. 1. Convergence of the e^+-H scattering length as a function of $\frac{1}{y_{max}}$. The extrapolated value corresponding to $y_{max} = \infty$ is $A_\infty = -2.108$.

displayed in Fig. 1 and justified by a pure $\frac{\alpha}{r^4}$ long range polarization potential.

By taking only the b_1 term we get $b_1 = 6.9$ and the value $A_\infty = -2.109$. By adding the quadratic term b_2 these results are only slightly modified, giving $A_\infty = -2.108$ close to the values -2.1036 ± 0.0004 given in [4] or -2.103 ± 0.001 in [6]. The coefficients of (38) in the quadratic interpolation are $b_1 = 6.6$ and $b_2 = 0.0016$.

Apart from the methodological difference, the calculations of [4,6] assumed an infinitely heavy proton whereas our results are obtained by the normal proton mass. This finite mass effect is responsible for the small difference between both approaches. For $N_c = 4$ it gives a correction of 0.004, leading to a full agreement with the most accurate variational calculations. Our final result is then $A_\infty = -2.108 \pm 0.001$ for a finite mass proton and $A_\infty = -2.104 \pm 0.001$ in the limit $m_p \to \infty$.

A final comment on that point could be of some interest. Let us first remark that in our approach no two-body polarization interactions are included. Our input is limited to the Coulomb potentials between different pairs and potential (37) was only considered as a guide in understanding the y_{max} dependence of the scattering length. The polarization effects are automatically generated by the dynamics of the Faddeev equations and contained in the b_i coeficients of expansion (38). Furthermore, in the asymptotic region, as far as the system is driven by a two-body potential such as (37), one has the identity $b_1 \equiv \sqrt{2}\alpha$. Thus the knowledge of b_1, obtained by directly solving the scattering Faddeev equations, provides an independent and direct evaluation of the atomic polarizability. The value we have found for this coefficient, $b_1 = 6.6 \pm 0.1$, corresponds to a polarizability $\alpha = 4.66 \pm 0.1$, in close agreement with its standard value $\alpha = 4.5$. The difference of a few percent between these two values falls inside the numerical uncertainties in the extraction of b_1 and cannot confidently be attributed to the proton finite mass effects.

A similar study provides us with the zero-energy effective density value $Z_{eff} = 8.91 \pm 0.01$, compatible with [6]. Figure 2 shows the density distribution (32) as function of the distance of the proton from the $e^+ e^-$ pair $\rho \simeq \frac{1}{2} y_2$ [see Eq. (5)]. It is seen that the main contribution into the 2γ annihilation rate comes from the domain around $\rho = 1.9 a_0$.

B. Elastic phase shifts

Our next results concern the e^+-H elastic phase shifts below the Ps($n = 1$) threshold, i.e., in the momentum

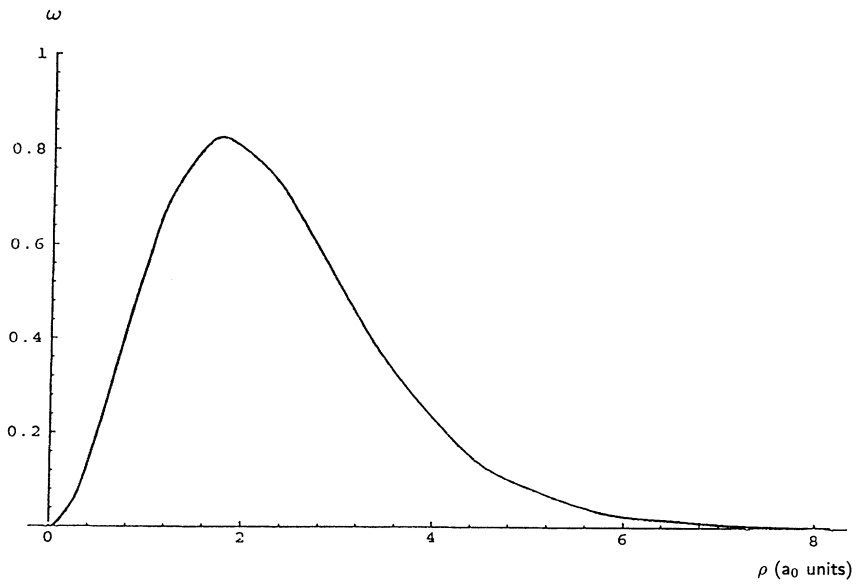

FIG. 2. Zero-energy density distribution (32) for the 2γ annihilation of the $e^+ e^-$ pair.

TABLE II. Phase shifts (in rad) of the s-wave e^+-H elastic scattering; k_1 is the momentum (19) of the incident positron.

$k_1(a_0^{-1})$	Present work	Ref. [5]	Ref. [10]
0.1	0.149	0.1483	0.152
0.2	0.188	0.1877	0.188
0.3	0.166	0.1677	0.166
0.4	0.120	0.1201	0.118
0.5	0.060	0.0624	0.061

TABLE III. Convergence of the K-matrix elements for $k_1 = 0.71a_0^{-1}$.

N_c	$\{l_1\}$	$\{l_2\}$	K_{11}	K_{12}	K_{22}
8	0123	0123	-0.062	-0.037	0.294
10	01234	01234	-0.060	-0.029	0.317
12	012345	012345	-0.058	-0.026	0.320
14	0123456	0123456	-0.057	-0.024	0.325
16	01234567	01234567	-0.058	-0.024	0.327

region $0 \leq k_1 \leq \frac{\sqrt{2}}{2}a_0^{-1} = 0.7071a_0^{-1}\ldots$. The results are summarized in Table II. They have been obtained by taking into account the $N_c = 10$ bipolar partial channels ($l_1 = 0,1,\ldots,4$ and $l_2 = 0,1,\ldots,4$). Their convergence as a function of N_c is faster than for zero energy. No polarization effects have been observed in the energies considered and we can simply conclude, in fair agreement with the variational results of Ref. [5] as well as with those of a more recent calculation [10], that the Schrödinger equation has been solved via a finite-element expansion.

C. Inelastic phase shifts

The most interesting results concern scattering within the ore gap $0.7071a_0^{-1} < k_1 < 0.8660a_0^{-1}$. Many calculations have been done in the past without any conclusive agreement [9]. The more firmly established results seems to be those of [7]. However, sensible disagreement was found in a recent calculation [15] and even in [16] for near threshold energies.

Table III shows the convergence of the near threshold ($k_1 = 0.71a_0^{-1}$) K-matrix elements with an increasing number of bipolar harmonics. The convergence is quite regular, but a bit slower than for the scattering length.

The energy dependence and cross sections have been calculated with $N_c = 16$. Results for k_1 in the interval $0.71a_0^{-1} - 0.85a_0^{-1}$ are given in Table IV. Except for the value $k_1 = 0.85a_0^{-1}$, to be discussed later, these values are in pretty good agreement with those of variational calculations [7].

A few percent disagreement for some values of the K-matrix elements can be attributed both to the contribution of higher partial channels in our calculations as well as to inaccuracies of the variational calculations [7] where the convergence of the nondiagonal element K_{12} is not quite achieved. Of course, discrepancies are magnified in the positronium formation cross section σ_{12}, but they remain at the 1% level in the region $k_1 \leq 0.80a_0^{-1}$.

In the interval $0.80a_0^{-1} < k_1 < 0.8660a_0^{-1}$ we observed for the positronium formation cross section the behavior displayed in Fig. 3. It corresponds to a sharp (note the logarithmic scale in Fig. 3) and narrow ($\Gamma \approx 0.2$ eV) resonance just below the n=2 hydrogen threshold. The existence of such a resonance was first found in [24] by

TABLE IV. K-matrix elements and elastic and positronium formation cross sections (20) (in units of πa_0^2).

k_1	Reference	K_{11}	K_{12}	K_{22}	σ_{11}	σ_{12}
0.71	this work	−0.059	−0.024	+0.33	0.027	0.0041
	[7]	−0.057	−0.024	+0.363	0.026	0.0041
	[15]				0.033	0.0034
0.75	this work	−0.085	−0.029	−0.54	0.050	0.0045
	[7]	−0.078	−0.028	−0.532	0.043	0.0044
	[15]				0.050	0.0038
	[16]	−0.078	−0.023			
0.80	this work	−0.109	−0.052	−1.52	0.071	0.0050
	[7]	−0.104	−0.051	−1.513	0.065	0.0049
	[15]				0.076	0.0043
	[16]	−0.169	−0.052			
0.85	this work	−0.169	−0.425	−6.40	0.108	0.0232
	[7]	−0.130	−0.126	−3.735	0.086	0.0058
	[15]				0.100	0.0049
	[16]	−0.277	−0.115			

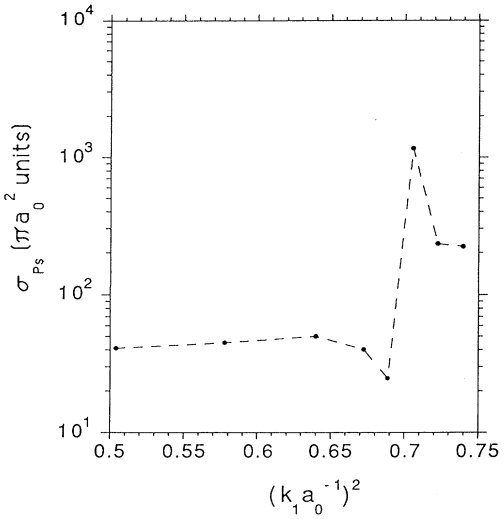

FIG. 3. Positronium formation cross section (in units of πa_0^2) below the n=2 hydrogen threshold.

using the coordinate rotation method and discussed later by many authors (see [15] and references therein). Our calculations confirm its existence in a direct solution of the Schrödinger equation. However, its precise structure, e.g., position and width, would require one to carefully scan the region covered in Fig. 3 with a very fine energy step. This is now beyond our computational availability.

V. CONCLUSION

We have presented a method to solve directly the e^+-H scattering problem without making use of any intermediate approximations. We have shown the reliability of the Faddeev approach in solving the Coulomb three-body problem. The method, based on a direct solution of the Schrödinger equation, provides accurate results and allows the study of long range polarization effects a well as near threshold resonances. The results look rather encouraging in view of possible applications of the method to study other Coulomb three-body processes with several open channels.

ACKNOWLEDGMENTS

We would like to thank Professor C. Wilkin and Professor J. W. Humberston for interesting and helpful discussions in the revised version of this manuscript.

[1] M. Charlton, Rep. Prog. Phys. **48**, 737 (1985).
[2] G. Spicher *et al.*, Phys. Rev. Lett. **64**, 1019 (1990).
[3] W. Sperber *et al.*, Phys. Rev. Lett. **68**, 25 (1992); **68**, 3690 (1992).
[4] S.K. Houston and R.J. Drachman, Phys. Rev. A **3**, 1335 (1971).
[5] A.K. Bhatia, A. Temkin, R.J. Drachman, and H. Eiserike, Phys. Rev. A **3**, 1328 (1971).
[6] J.W. Humberston and J.B.G. Wallace, J. Phys. B **5**, 1138 (1972).
[7] J.W. Humberston, J. Phys. B **17**, 2353 (1984).
[8] E.A.G. Armour and J.W. Humberston, Phys. Rep. **204**, 165 (1991).
[9] J.W. Humberston, Adv. At. Mol. Opt. Phys. **32**, 205 (1994).
[10] F.S. Levin and J. Shertzer, Phys. Rev. Lett. **61**, 1089 (1988).
[11] A.A. Kvitsinsky and C.-Y. Hu, Few-Body Syst. **12**, 7 (1992); C.-Y. Hu and A.A. Kvitsinsky, Phys. Rev. A **46**, 7301 (1992).
[12] A.A. Kvitsinsky, J. Carbonell, and C. Gignoux, Phys. Rev. A **46**, 1310 (1992).
[13] A.A. Kvitsinsky and C.-Y. Hu, Phys. Rev. A **47**, 994 (1993); **47**, R3476 (1993).
[14] S.P. Merkuriev, Ann. Phys. (N.Y.) **130**, 395 (1980).
[15] B.J. Archer, G.A. Parker, and R.T. Pack, Phys. Rev. A **413**, 1303 (1990).
[16] U. Roy and P. Mandal, Phys. Rev. A **48**, 233 (1993).
[17] S.P. Merkuriev, C. Gignoux, and A. Laverne, Ann. Phys. (N.Y.) **99**, 30 (1976).
[18] A.A. Kvitsinsky, V.V. Kostrykin, and S.P. Merkuriev, Fiz. Elem. Chastits At. Yadra **21**, 1301 (1990) [Sov. J. Part. Nucl. **21**, 553 (1990)].
[19] C.R. Chen, G.L. Payne, J.L. Friar, and B.F. Gibson, Phys. Rev. C **31**, 2266 (1985); **39**, 1261 (1989).
[20] N.W. Schellingerhout, L.P. Kok, and G.D. Bosveld, Phys. Rev. A **40**, 5568 (1989).
[21] P.M. Prenter, *Splines and Variational Methods* (Wiley, New York, 1975).
[22] G.L. Payne, in *Models and Methods in Few-Body Physics*, edited by L. S. Ferreira *et al.*, Lecture Notes in Physics Vol. 273 (Springer-Verlag, Berlin, 1987), p. 64.
[23] J. Carbonell, C. Gignoux, and S.P. Merkuriev, Few-Body Syst. **15**, 15 (1993).
[24] G.D. Doolen, J. Nuttall, and C.J. Wherry, Phys. Rev. Lett. **40**, 313 (1978).